Charge Transfer and Energy Level Alignment at the Interface between Cyclopentene-Modified Si(001) and Tetracyanoquinodimethane

ARTICLE *in* THE JOURNAL OF PHYSICAL CHEMISTRY C · SEPTEMBER 2014

Impact Factor: 4.77

1 AUTHOR:

Anzar Khaliq

Habib University

5 PUBLICATIONS **13** CITATIONS

THE JOURNAL OF PHYSICAL CHEMISTRY C

Article

pubs.acs.org/JPCC

Charge Transfer and Energy Level Alignment at the Interface between Cyclopentene-Modified Si(001) and Tetracyanoquinodimethane

Anzar Khaliq,[§,‡] Jean-Jacques Gallet,[†,§] Fabrice Bournel,[†,§] Debora Pierucci,[†,§] Héloïse Tissot,[†,§] Mathieu Silly,[†] Fausto Sirotti,[†] and François Rochet*[,†,§]

[§]UMR 7614, Laboratoire de Chimie Physique, Matière et Rayonnement, UPMC Univ Paris 06, Sorbonne Universités, 11 rue Pierre et Marie Curie, 75231 Paris Cedex, France

[†]Synchrotron SOLEIL, L'Orme des Merisiers, Saint-Aubin, BP 48, 91192 Gif sur Yvette Cedex, France

[‡]Habib University Foundation, 147, Block 7 & 8 Banglore Cooperative Housing Society, Tipu Sultan Road, Karachi 75350, Pakistan

Supporting Information

ABSTRACT: We examine how the electronic structure (via synchrotron radiation XPS, UPS, and NEXAFS) and the molecular orientation (via NEXAFS) of a strong acceptor molecule, tetracyanoquinodimethane (TCNQ), change as a function of thickness when it is deposited on the cyclopentene-covered Si(001)-2×1 substrate. XPS shows that the monomolecular cyclopentene layer acts as an efficient chemical protective barrier. All spectroscopies indicate that anionic TCNQ is formed at (sub)monolayer coverage. However, the transfer should only concern those CN moieties pointing toward the Silicon surface. At higher thicknesses, neutral TCNQ is observed. We do not observe the upward bending of the silicon bands associated with electron transfer from the substrate to the acceptor molecular that one would expect for an unpinned Fermi level interface. In fact, donor levels are likely created within the cyclopentene layer or at its interface with silicon. The formation of $TCNQ^-$ is associated with a strong increase in the work function. The attained value (~5.7 eV) is independent of the work function of the cyclopentene-modified Si(001) surface (that varies with Si doping), in agreement with the integral charge transfer model. Therefore, ultrathin layers of TCNQ can be used to improve the hole-injection properties of this alkene-modified silicon surface.

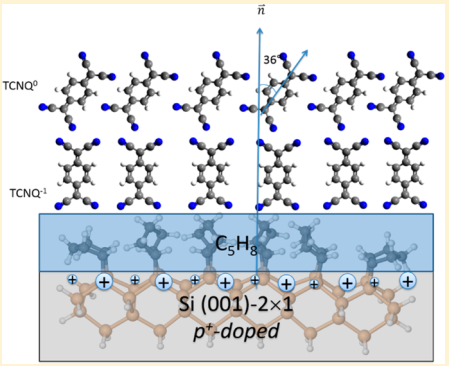

INTRODUCTION

Charge transfer between inorganic semiconductors (ISCs) and strong acceptor molecules deposited on their surfaces has recently attracted much attention, due to its relevance to (opto)electronic device technology.[1−3] It offers an elegant way to control the carrier concentration in nanostructured ISC materials for which dopant implantation is impractical.[1−3] Enhancement of the surface work function of ISCs enables their optimization as hole injectors.[4,5] Charge transfer is also a key issue in sensor science involving modified surfaces of ISCs.[6]

The principles of ISC surface-transfer doping have been reviewed by Chen and co-workers.[1] According to those authors, when an acceptor molecule has its electron affinity (EA) in the solid state larger than the ionization potential (IP) of the substrate, then electron charge is transferred spontaneously from the substrate to the molecule.[1] Otherwise stated, charge transfer occurs when, before level alignment, the lowest unoccupied molecular orbital (LUMO) of the acceptor lies below the valence band maximum (E_{VB}) of the ISC.

Nevertheless, the straightforward use of concepts like the energy positioning of the LUMO, or the EA in the molecular solid, that are then compared to the substrate IP, seems too schematic and therefore may not be predictive. This prompted Braun, Salaneck, and Fahlman to propose the integer charge transfer (ICT) model,[7] in which the negative ICT state (ICT^-) energy is distinct from the EA. As discussed by Bokdam et al.,[8] the ICT^- level does not coincide with the EA of the solid organic material (often larger than EA by ~1 eV) due to electrostatic interactions at the interface. For acceptor molecules weakly interacting with the substrate (i.e., making no covalent bonds), the ICT^- is the energy gained when one electron is added to the molecule, producing a fully relaxed state. When ICT^- is smaller than the substrate work function Φ_{sub}, a simple thermodynamic argument shows that this level cannot be filled by electrons coming from substrate. Then vacuum-level alignment is observed (the so-called Schottky−Mott limit). On the other hand (what is expected for strong acceptors), charge transfer occurs—i.e., a layer of molecular anions forms at the interface—when the ICT^- energy is larger than Φ_{sub}. Then the Fermi level in the substrate and the ICT^- level in the molecular solid align. Associated with this Fermi-level pinning, an electrostatic potential step occurs at the

Received: March 18, 2014
Revised: September 5, 2014
Published: September 8, 2014

   dx.doi.org/10.1021/jp502680b | J. Phys. Chem. C 2014, 118, 22499−22508

interface, resulting in an increase in work function. *Therefore, in the Fermi-level pinning case, the work function of the acceptor layer/substrate system is a measure of ICT*$^-$. Bokdam et al.[8] have shown that the value of ICT$^-$ is a property of the acceptor molecule layer only, independent of the substrate.

Charge transfer to the acceptor molecule means that the positive charges are left in the substrate to preserve overall charge neutrality. In the specific case of ISC substrates, the electric field created by this dipolar layer may induce an upward band bending, leading to hole accumulation.[1,2,9] Although not stated explicitly in ref 1, hole accumulation requires that the Fermi level at the ISC is unpinned; i.e., there is an extremely low density of surface states in the gap, below 10^{-3} of a monolayer (ML).[10−12]

A spectacular illustration of charge-transfer doping is provided by the deposition of tetrafluorotetracyanoquinodimethane (F4-TCNQ) on top of *p*-doped hydrogenated diamond C(001)-2×1 (H-C(001)-2×1), an electronically well-passivated surface. F4-TCNQ deposition induces an upward band bending (accumulation), leading the formation of a high areal density of holes.[1,2] Chen and co-workers[1,2] argue that charge transfer occurs because the EA of solid F4-TCNQ (EA = 5.24 eV[13]) is larger than the IP of H-C(001)-2×1 (4.4 eV). On the same surface, tetracyanoquinodimethane (TCNQ) with EA = 4.0 eV,[14] has a weaker *p*-doping efficiency (manifested by a small upward band bending) compared to that of F4-TCNQ. This is rationalized in refs 1 and 2 on the basis of the EA of TCNQ, which is now slightly greater than the hydrogenated diamond IP. Electron transfer is also documented between H-terminated Si(111)-1×1 and acceptor molecules (F4-TCNQ,[3] tetracyanoethylene[6]). Like H-terminated C(001)-2×1, H-terminated Si(111)-1×1 is a well-passivated surface with an extremely low density of gap states.[15]

As an alternative to H-termination, silicon surfaces can be terminated by an organic buffer layer that is thought to be more effective to protect the silicon from chemical reactions with the molecular acceptor.[16] Well (electronically) passivated Si(111) surfaces in nearly flat band conditions can be obtained via wet chemistry, for instance, the methylated surface.[17] However, the wet chemistry route is not practicable for the Si(001)-2×1 surface, and an organic termination is obtained via the reaction of π-bonded molecules, in particular alkene molecules, with the silicon dimers.[18,19] The present work aims at providing further experimental data on charge transfer between silicon and an acceptor molecule across a monomolecular alkene buffer layer. In the wake of a preceding work devoted to the adsorption geometries of cyclopentene on Si(001)-2×1,[20] we examined, via synchrotron radiation, the electronic structure of TCNQ overlayers deposited on the cyclopentene-modified Si(001) surface (CP-Si(001)-2×1). Cyclopentene was already used as an efficient chemical buffer layer, facilitating the crystalline growth of pentacene molecules.[21] Aware that the question of electrically active defects possibly left after cyclopentene layer formation are critically important, we used Si(001) substrates with two extreme doping levels (n^+ and p^+) to examine the issue of Fermi level pinning. The deposition of TCNQ on CP-Si(001)-2×1 was followed by synchrotron radiation ultraviolet photoelectron spectroscopy (UPS), X-ray photoelectron spectroscopy (XPS), and N 1s near-edge X-ray fine structure spectroscopy (NEXAFS). Information is gathered on chemical environments, molecular charge state, molecular orientation, energy level offsets at the interface, and changes in work function. This enabled us to draw a picture of the TCNQ/CP-Si(001)-2×1 interface energetics and to discuss it in terms of the existing models.[1,7] Possible applications of ultrathin TCNQ film in solar cells based on silicon/organics interfaces are also discussed.[22−24]

EXPERIMENTAL SECTION

Sample Preparation. Si(001)-2×1 surfaces were produced in the preparation chamber of the TEMPO beamline end-station at SOLEIL synchrotron facility. Two differently doped silicon substrates (phosphorus-doped n^+-type Si(001) wafers with a resistivity of 0.003 Ω·cm, $N_D \approx 2 \times 10^{19}$ cm^{-3}, and boron-doped p^+-type Si(001) wafers with a resistivity of 0.002 Ω·cm, $N_A \approx 5.7 \times 10^{19}$ cm^{-3}) were cleaned from their native oxide by flash annealing (Joule effect) at 1100 °C after prolonged degassing at 600 °C in ultrahigh vacuum (10^{-10} mbar base pressure).

The clean silicon surface was first exposed to 6.75 L of cyclopentene by dosing for 15 min at room temperature under a pressure of 10^{-8} mbar (ion gauge uncorrected reading). Doses are expressed in Langmuir (1 L = 10^{-6} Torr·s). Cyclopentene was purified by several freeze−pump−thaw cycles before dosing. In ref 20, we showed that the majority of cyclopentene molecules attach to the silicon dimer without dissociation via a cycloaddition-like reaction. However, we have also found evidence for a minority product, resulting from an ene-like reaction, not detected in previous studies,[25,18] and whose proportion increases with increasing deposition temperature. The C 1s XPS spectrum of the starting CP-Si(001)-2×1 surface (on which TCNQ is deposited) is that published in ref 20 as Figure 2a (corresponding to substrate temperatures ≤130° during exposure to cyclopentene).

TCNQ was evaporated through a crucible whose back was heated by a filament. A thick film (∼10^{15} molecules/cm^2) was deposited on n^+-doped CP-Si(001). Deposits in the range 10^{14}−10^{15} TCNQ molecules/cm^2 were obtained for p^+-doped CP-Si(001). The methodology adapted to estimate the molecular thickness for both thin and thick layers is explained in section S1 of the Supporting Information

Synchrotron Radiation Spectroscopies: X-ray Photoemission. The X-ray spot (normally focused in a spot 45 μm long in the horizontal direction by 10 μm wide in the vertical dimension) was defocused on purpose, to a spot of dimensions 1 mm × 2 mm, to reduce beam damage, without losing photoelectron count rate. All photoemission spectra were taken with a takeoff angle of 35° with respect to the surface normal. Valence band UPS spectra were recorded at $h\nu$ = 60 eV, while surface sensitive Si 2p spectra were measured at $h\nu$ = 150 eV, with an overall experimental resolution better than 80 meV. The precision on the Si $2p_{3/2}$ binding energies of the bulk component is better than 10 meV. N 1s core-level XPS spectra were recorded at $h\nu$ = 450 eV with an overall experimental resolution better than 100 meV. After subtraction of a Shirley background, the N 1s spectra were reconstructed with sums of Voigt functions, whose Lorentzian full-width at half-maximum (fwhm) was fixed to 0.12 eV, and the Gaussian fwhm was set as a free fitting parameter.

To quantify the amount of deposited molecule, N 1s spectra were recorded at $h\nu$ = 530 eV, at a kinetic energy (KE) of about 132 eV, close to that of the Si LVV Auger peak (∼80−88 eV range). The N 1s photoemission peak integrals were normalized with respect to an equal Si LVV height. The values were compared to the N 1s spectrum for a NH_3 saturated silicon surface recorded close to the Auger peak and normalized

dx.doi.org/10.1021/jp502680b | J. Phys. Chem. C 2014, 118, 22499−22508

in the same way as mentioned above. Si(001)-2×1 completely saturated by NH_3 corresponds to a coverage of half a monolayer, i.e., 3.4 × 10^{14} atoms/cm^2.[26] A linear relation between N 1s intensities and N surface coverage is expected for deposits in the monolayer range. For multilayer films, the TCNQ surface density was estimated from the N 1s to Si 2p ratio measured at $h\nu$ = 450 eV (see Supporting Information, Figure S1).

Work Function Measurements. The work function is measured via the kinetic energy of the secondary electron cutoff (KE_{cutoff}). With the knowledge of the kinetic energy of the Fermi level (KE_{Fermi}) and a precise determination of the photon energy $h\nu$, one gets the work function ,Φ: $\Phi = h\nu - (EK_{Fermi} - EK_{cutoff})$ (see Supporting Information, Figure S2). The precision in measuring Φ is 10 meV.

NEXAFS Spectroscopy. N 1s NEXAFS spectra of the adsorbed layer were recorded at different angles θ, between the normal to the sample surface and the polarization vector $\vec{E}$, in the range from 6° (grazing incidence) to 90° (normal incidence). The orientation of the molecular orbital final state was derived using these normalized spectra (see Supporting Information, Figures S5 and S6).[27]

RESULTS AND DISCUSSION

Cyclopentene-Covered Si(001)-2×1 Surface (CP-Si(001)). The Si 2p$_{3/2}$ binding energy (BE) of the pristine p^+-doped CP-Si(001) surface is 99.12 eV, see Figure 1a. This corresponds to an energy difference between the Fermi level (E_F) and the valence band maximum (E_{VB}), $E_F - E_{VB}$ = 0.38 eV, assuming an energy difference E_{VB} − BE(Si 2p$_{3/2}$) = 98.74 eV.[11] Therefore, after cyclopentene adsorption on p^+-doped CP-Si(001), bands are bent downward by 0.38 eV (due to high doping, the Fermi level coincides with E_{VB} in the bulk). For the n^+-substrate (Figure 1b), the Si 2p$_{3/2}$ of CP-Si(001) is at 99.42 eV, corresponding to an energy difference $E_F - E_{VB}$ = 0.67 eV. In that case, the bands are bent upward by 0.44 eV, given that the Fermi level is aligned with the conduction band minimum E_{CB} in the bulk (we take a gap energy $E_{CB} - E_{VB}$ = 1.12 eV).

Comparison of p^+ and n^+ CP-Si(001) surfaces shows that the Fermi level position within the gap measured with respect to E_{VB} varies within the energy interval from 0.38 eV (p+) to 0.68 eV (n^+). This indicates the presence of donor and acceptor defect levels at the surface.

A negative (positive) charge appears at the surface for the n^+ (p^+) sample, as well as a positive (negative) space charge layer in the silicon. This is a marked difference with the H-C(001)-2×1 and H-Si(111)-1×1 cases, for which the Fermi level is completely unpinned at the surface, leading to flat band conditions. The work function, measured with an accuracy of ±0.05 eV (see also Supporting Information, Figure S2), is 4.51 eV for the p^+ and 3.92 eV for the n^+, a very substantial reduction with respect to the clean Si(001) case, viz., 5.02 eV for p^+ and 4.80 eV for n^+.

TCNQ Deposition on p^+-Doped and n^+-Doped CP-Si(001). Upon deposition of successive TCNQ layers on p^+-doped CP-Si(001)-2×1 substrate, the line shape of the Si 2p spectrum is not much affected, as shown in Figure 1a. The spectra are slightly broadened due to the growth of a small component, shifted by +0.25 eV from the bulk line. However, the chemical BE shift is too small to be attributed to the formation of Si−O (due to oxygen/water contamination)[28] or Si−N covalent bonds (core level shift in the range from +0.8 to +0.9 eV).[26,29] The origin of this component remains elusive. A

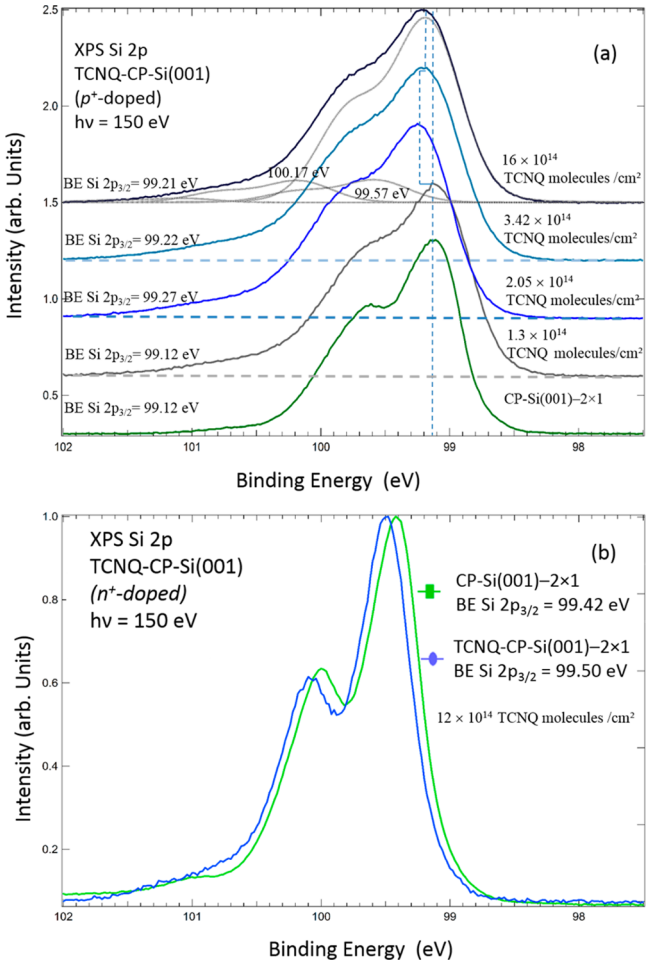

Figure 1. (a) Evolution of Si 2p spectra, from sub-monolayer coverage to a thick layer of TCNQ deposited on p^+-doped CP-Si(001). (b) Si 2p spectra of n^+-doped CP-Si(001) before and after deposition of a thick layer of TCNQ (~12 × 10^{14} TCNQ molecules/cm^2).

small oxidation peak (Si^+)[28] appears, shifted by about +0.9 eV from the bulk component, maybe due to contamination by oxygenated species during TCNQ deposition in the preparation chamber. From the second deposition onward (from 2 × 10^{14} molecules/cm^2 to a "thick" layer of 16× 10^{14}), we see that the Si 2p$_{3/2}$ BE slightly increases, falling in the 99.21−99.27 eV range, corresponding to a $E_F - E_{VB}$ energy difference of ~0.50 eV. Therefore, the downward band bending has slightly increased (by ~0.1 eV) with respect to the pristine p^+ CP-Si(001) case.

For the n^+ sample, for which only one thick deposition was made (~12 × 10^{14} molecules/cm^2), we do not observe any broadening of the Si 2p components after TCNQ deposition (Figure 1b). The sole effect of TCNQ deposition is a rigid shift of the Si 2p spectra, as the Si 2p$_{3/2}$ binding energy increases to 99.50 eV, corresponding to an $E_F - E_{VB}$ energy difference of 0.76 eV. Thus, for the n^+ sample the upward band bending slightly decreases (by ~0.1 eV) after TCNQ deposition.

Therefore, for TCNQ deposition on both types of samples (p^+ and n^+), the observed band bending trends are opposite to what is expected when electron charge is transferred from silicon to the acceptor molecule.

Upon formation of the silicon cyclopentene interface the Fermi level is at about mid-gap. This corresponds to an upward band bending for the n^+ sample and a downward band bending

dx.doi.org/10.1021/jp502680b | J. Phys. Chem. C 2014, 118, 22499−22508

for the p^+. If electrons were transferred from silicon to TCNQ, the upward band bending (in absolute value) should have increased for the n^+ leading eventually to inversion. While for the p^+, the downward band bending (in absolute value) should have decreased (reverting into an upward band bending) leading to hole accumulation. This is also indicated by the band energy diagram in Figure 5, below. It seems that the deposition of TCNQ slightly diminishes the surface density of acceptor/donor defects formed at the interface between silicon and cyclopentene, leading to "flatter" band conditions. Because of a large density of interfacial states (greater than 10^{-3} ML), the behavior of CP-Si(001) contrasts with that of *p*-doped H-C(001)-2×1 for which the Fermi level is unpinned. Indeed, F4-TCNQ deposition leads to hole accumulation.[12]

Let us now consider the evolution of TCNQ electronic structure as a function of coverage which is followed by N 1s XPS performed at $h\nu$ = 450 eV. We first examine the XPS N 1s spectra of the thick layers deposited on p^+-doped and n^+-doped CP-Si(001) with coverages of 16 × 10^{14} and 12 × 10^{14} molecules/cm^2, respectively. The spectra given in Figure 2

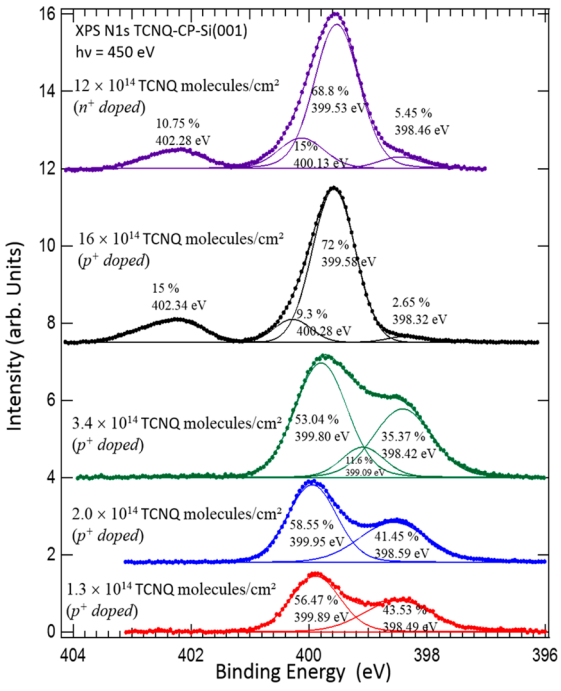

Figure 2. Evolution of N 1s spectra, from sub-monolayer coverage to a thick layer of TCNQ (~16 × 10^{14} TCNQ molecules/cm^2) deposited on a p^+-doped CP-Si(001)-2×1 substrate. The top curve is the N 1s spectrum of a thick TCNQ layer (~12 × 10^{14} TCNQ molecules/cm^2) deposited on an n^+-doped CP-Si(001)-2×1 substrate.

are characteristic of the molecular solid. For both types of substrates, they look almost identical in terms of shape. The N 1s spectrum is composed essentially of two N 1s components separated by 2.7 eV, in accord with previous reports,[30−33] a main line and a satellite at high BE, attributed to an intramolecular electronic excitation (HOMO-to-LUMO shake-up;[34] see also Figure S3 in the Supporting Information). For both samples, the BEs of the most intense N 1s components are practically the same within 0.05 eV, 399.58 eV for p^+ and 399.53 eV for n^+, indicating that the substrate doping has no measurable effect on the N 1s BE of the TCNQ thick layers. However, two small components at ~398.4 and ~400.2 eV need to be introduced to acquire a reasonable fit. Notice that they are more intense for n^+ than for p^+, the latter having a larger TCNQ coverage. In fact, these two peaks are attributed to interfacial components damped by the molecular solid overlayer. Let us now consider the series of spectra acquired for (sub)monolayer TCNQ coverages (in the 10^{14} molecules/cm^2 range) on p^+-doped CP-Si(001)-2×1 that enables us to describe the formation of the interface. As it can be seen in Figure 2, the spectral shape is noticeably different from that of the thick layers. The low-coverage spectra exhibit two components.

The lower BE component (398.4 eV) matches with the N 1s BE of anionic TCNQ or F4-TCNQ; see, for instance, TCNQ on Ni (111) (398.1 eV)[35] and on Cu(001) (398.7 eV),[36] and F4-TCNQ on graphene (398.3 eV)[37] and on H-C(001)-2×1 (397.5 eV).[2] The BE of the second component (~399.9 eV) is close (but not equal) to that of the thick, neutral, TCNQ^0 layer (399.6 eV). Its attribution to *ground-state* TCNQ^0 is not that obvious. Indeed, despite its representation of more than half the spectral weight (about 57% for a molecular coverage of 1.3 × 10^{14} molecules/cm^2), we do not see any shakeup at ~402 eV, which suggests that the LUMO is filled. Note that this is also the case for anionic TCNQ on Cu(100).[36] The formation of neutral TCNQ molecules farther away from the interface in growing molecular crystallites may be incipient for the deposit equal to 3.4 × 10^{14} molecules/cm^2, for which a third, small component at 399.1 eV needs to be introduced. We shall see that the assumption of charged and neutral species coexisting on the surface for deposits in the 10^{14} molecules/cm^2 range is inconsistent with the N 1s NEXAFS spectra.

We start with the N 1s NEXAFS spectra of a thick TCNQ deposit (16 × 10^{14} TCNQ molecules/cm^2 on p^+-doped CP-Si(001)-2×1 sample) shown in Figure 3a, measured for various angles θ between the surface normal $\vec{n}$ and the polarization vector $\vec{E}$ of the radiation (the NEXAFS spectra of the thick film deposited on the n^+-doped CP-Si(001) substrate, presented in Supporting Information, Figure S4, are identical to that deposited on the p^+ one). The thick film is characteristic of neutral TCNQ. We observe three main peaks, labeled 1, 2, and 3, which present a dichroic behavior. The transition energies are comparable to the ones published in the literature.[33,36,38] To interpret these spectra, we follow, at least in part, the arguments of Fraxedas et al.[33] Those authors performed a DFT calculation of the energies of the unoccupied Kohn−Sham orbitals and then simply shifted the experimental spectra on their calculated energies to identify the transitions. Indeed, with the creation of the core-hole, there is no reason why the energy difference between Kohn−Sham orbitals (see Supporting Information, Figure S3) should remain the same, as discussed in ref 39. This crude approach leaves the 1s-to-LUMO b_{2g} transition apart (which nonetheless is allowed) without further justification. Resonances 1 and 3 are attributed to transitions to orbitals which are all perpendicular to the molecular plane ($\pi_\perp$*). Peak 1 at 396.95 eV originates from the lower a_u and b_{1u} orbitals of TCNQ (pertaining to the central ring),[33] to which we add the LUMO b_{2g} (Supporting Information, Figure S3), also of $\pi_\perp$* type and distributed all over the molecule, including the cyano groups. Peak 3, present at 399.92 eV, arises from the π orbital delocalized all over the molecule and originates from a b_{2g} symmetry orbital. Peaks 1 and 3 have maximum intensity for grazing incidence when the electric field is perpendicular to the surface.

dx.doi.org/10.1021/jp502680b | J. Phys. Chem. C 2014, 118, 22499−22508

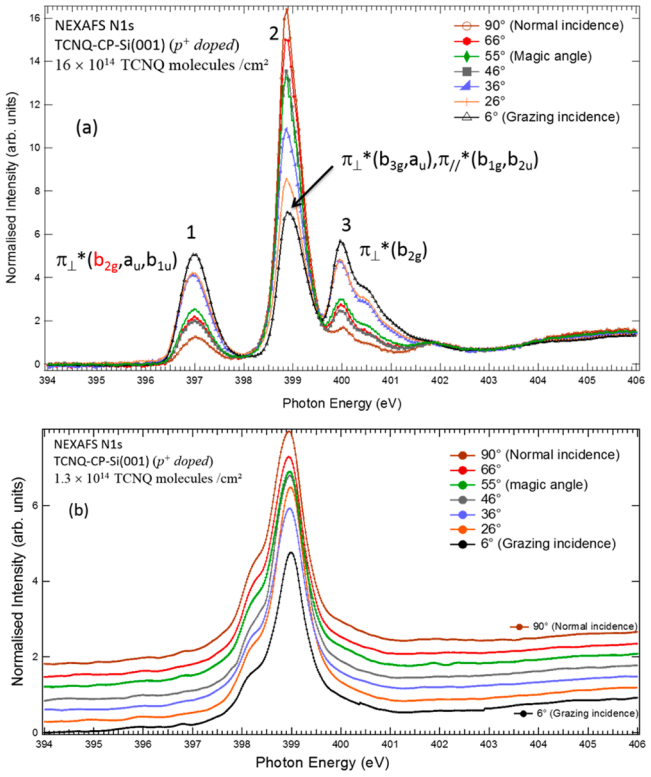

Figure 3. Angle-dependent N 1s NEXAFS spectra of TCNQ deposits on p^+-doped CP-Si(001)-2×1 of (a) a thick layer of TCNQ (16×10^{14} TCNQ molecules/cm^2) and (b) a sub-monolayer coverage (1.3×10^{14} TCNQ molecules/cm^2). θ is the angle between the surface normal $\vec{n}$ and the polarization vector $\vec{E}$ of the radiation.

Peak 2 situated at 399 eV encompasses contributions from four orbitals of TCNQ localized on the C≡N that are both perpendicular (⊥) and parallel (||) to the molecular plane.[33] The π^* transitions associated with the two orbitals perpendicular to the molecular plane ($\pi_\perp^*$) are b_{3g} and a_u, while the transitions from the orbitals parallel to the molecular plane are labeled b_{1g} and b_{2u}. Peak 2 is highly intense for normal incidence when the electric field is parallel to the surface. The higher lying weak components present above the IP (405.23 eV) correspond to transitions to σ^*(C−C), σ^*(C−H), and σ^*(C≡N) orbitals. The molecular orientation of TCNQ in the thick layer can be measured by analyzing the intensity dependence of resonances with the angle θ between the polarization vector $\vec{E}$ and the surface normal for the unoccupied states with the N 2p-axis perpendicular to the molecular plane such as peak 1 (a_u, b_{1u}). The angle α between the normal to the surface and the normal to the molecular plane is found equal to ∼36° using the method given in ref 40 (see Supporting Information, Figure S5).

Figure 3b presents angle-dependent NEXAFS spectra for a thin layer (molecular coverage of 1.3×10^{14} TCNQ molecules/cm^2). The spectra are taken for various angles θ specified on the graph. The NEXAFS spectra are markedly different from those of the thick film (Figure 3a). A doublet is observed at photon energies of 398.2 and 399 eV, that likely derives from the two degenerate and orthogonal N 1s-to-"cyano localized π^*" transition of the molecular solid (peak 2, 399 eV). In fact, the most striking observation is the absence of any transition at around 397 eV, the peak 1 of the neutral molecular solid (1s-to-$\pi^*_\perp$, including the LUMO b_{2g}). This is a general observation for anionic TCNQ, e.g., TCNQ on Cu(001).[36] If both neutral and charged species in comparable amounts were coexisting on the surface, then we should observe perforce in the NEXAFS spectra the peak at 397 eV characteristic of $TCNQ^0$. As the transition at 397 eV is missing, and the shakeup characteristic of $TCNQ^0$ is quenched in the N 1s XPS spectra of Figure 2, we must abandon the possibility of having some molecules in the neutral state, and some other charged, as N 1s XPS spectrum may suggest.

The (weak) angle dependence of the doublet at 398.2 and 399 eV can be used to discuss the molecular orientation at sub-monolayer coverage. The relative ratio of the two components is approximately constant (∼2.8) with varying θ. This is an indication that the molecule does not lie flat on the surface, otherwise their angular-dependence should show opposite trends. As these two components correspond to transitions to two orthogonal π^* orbitals, the C≡N π system is of the "plane type" according to Stöhr's nomenclature.[40] The angle γ between the C≡N axis of the molecule and the surface normal can be determined from the angular dependence of the *sum* of the absorption peak intensities at $h\nu$ = 398.9 and 398.2 eV. γ is found to be about 50° (see Supporting Information, Figure S6). This value is close to the magic angle (54.7°), which explains why the intensity is weakly dichroic. Considering the molecular structure of TCNQ published in the literature,[41] a molecule with its long axis normal to the surface has its C≡N bond axis at 57.6° from the surface normal. Conversely if the molecule sits with its long axis parallel to the surface and its molecular plane perpendicular to the surface then the C≡N bond axis should be at about 31° from the surface normal. The fitting value of γ (50°) suggests that the molecule stands upright with its long axis perpendicular to the surface. A crude estimate of the maximum monolayer coverage with molecules standing up in the trench separating two dimer row is about one molecule per $p(2\times2)$ cell, or 1.7×10^{14} molecules/cm^2. This compares with N 1s XPS indicating that the deposits affected by charge transfer are in the range 1×10^{14}–3×10^{14} molecules/cm^2. The orientational geometry of the molecule may be a clue for the puzzling observation of two N 1s XPS components in the (sub)monolayer range that points to two nonequivalent cyano pairs. For a standing up molecule, an initial state effect can be proposed. The molecule could be *asymmetrically charged*, with the lower part (the CN directed to the surface) getting more charge from the substrate than the upper part (the CN protruding into the vacuum). Note that the distribution of neutral to negative CN, 57:43, is close to, but not exactly equal to 50:50, as it would be expected for a standing up molecule. One cannot exclude electron diffraction effects we have not studied in detail, or variations in the N 1s photoionization cross section between neutral and charged CN. Alternately, one could assume that some molecules "touch" the modified silicon surface by only one CN to explain the excess of neutral CN N 1s signal.

The present observation is not isolated. Yoshimoto and co-workers have recently published the N 1s XPS and NEXAFS spectra of a F4-TCNQ sub-monolayer deposited on ethylene-modified Si(001).[5] The first N 1s NEXAFS resonance at 397 eV of the neutral molecule (seen for a thick layer) is suppressed, but two peaks at ∼400 and ∼399 eV (63%) with a 37:63 distribution are seen in the N 1s XPS spectrum. To explain the ratios, Yoshimoto and co-workers consider that most molecules are tilted with asymmetric charging, but some lie down on the surface with symmetric charging.

dx.doi.org/10.1021/jp502680b | J. Phys. Chem. C 2014, 118, 22499−22508

Figure 4 shows the UPS valence band spectra acquired at 60 eV for increasing coverage of TCNQ (from 1.3 × 10^{14} to 16 × 10^{14} molecules/cm^2) on p^+-doped CP-Si(001) and for the thick layer deposited on n^+-doped CP-Si(001) (12 × 10^{14} molecules/cm^2).

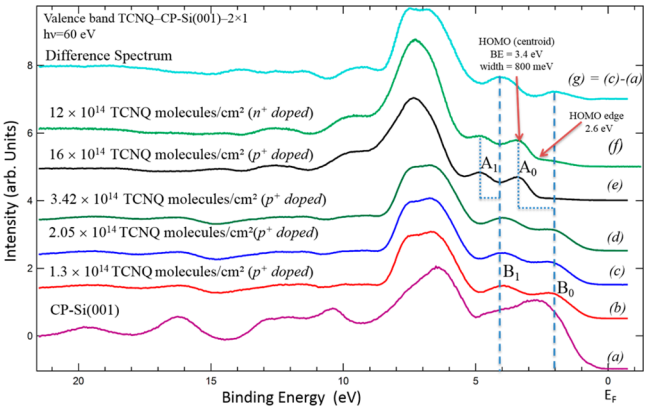

Figure 4. (a–e) Valence band of TCNQ for increasing coverage deposited on p^+-doped CP-Si(001)-2×1 substrate and (f) valence band of TCNQ thick layer deposited on n^+-doped CP-Si(001)-2×1 surface. (g) Difference spectrum between TCNQ and the CP-Si(001)-2×1 substrate.

We begin with the thick-layer case, which can receive a straightforward interpretation, as it is representative of neutral TCNQ. For both substrates, the HOMO (peak A_0), located at 3.4 eV (centroid), is followed by a second molecular component (HOMO−1, peak A_1) centered at 4.8 eV. This confirms that for thick TCNQ layers the HOMO binding energy does not depend on substrate doping. One can then search for evidence of a charge transfer in the valence bands at low coverage that parallels the N 1s XPS and NEXAFS observations. In the range 1.3 × 10^{14}–3.4 × 10^{14} molecules/cm^2 (Figure 4b–d), a new feature labeled B_1 shows up, centered at 4.0 eV. This molecular component is clearly distinct from the HOMO (peak A_0)/HOMO−1 (peak A_1) lines at 3.4 and 4.8 eV in the thick-film spectrum (Figure 4e,f). Another low-lying energy structure, labeled B_0, has appeared but as it merges with the Si valence band, its binding energy is more difficult to determine from the raw spectra. To emphasize the TCNQ contribution in the valence band, we subtract the substrate signal (curve a) to the (sub) monolayer spectrum (curve c) to give the difference curve f (see Supporting Information, Figure S7). A new feature B_0 appears at a BE of 2 eV.

The observation of the low-lying components B_0 and B_1 at ∼2 and ∼4 eV, respectively, is reminiscent of previous UPS studies related to systems which contain the anionic forms of TCNQ and F4-TCNQ.[2,4,42−46] In the case of solid K^+TCNQ^-,[44] which is essentially composed of the anionic form, Grobman et al. found three features at binding energies of ∼1.0, ∼2.0, and ∼4.2 eV, while the HOMO neutral solid TCNQ was found by those authors at ∼3 eV. Indeed, the presence of an unpaired electron in the LUMO-derived orbital causes a strong perturbation of the energies of the valence electronic levels.[46] The new B_0 and B_1 states observed can be assigned to the electrons in a LUMO-derived state and a HOMO-derived state.[46] Note that Masuda et al.[47] proposed an alternative explanation, the lowest binding energy peak B_0 being interpreted as the $TCNQ^0$ *lowest energy* (singlet) final state, following the valence ionization of $TCNQ^-$, and the second peak B_1 attributed to a shakeup, corresponding to the lowest-lying triplet excited state of the neutral molecule. The work functions Φ were also measured (see Supporting Information, Figure S2) for increasing amounts of TCNQ deposited on p^+-doped CP-Si(001) (reported in Table 1; see also Figure 5a). A huge increase (+1.5 eV) of the work function (from 4.51 to 5.91 eV) is already seen after the first deposit of 1.3 × 10^{14} molecules/cm^2. Given that the Fermi level moves by less than 0.1 eV, most of the work function change is due to the formation of a dipole layer with positive charge surface states inside and negatively charged TCNQ molecules outside. Notice that Mukai et al. make similar observation[4] for F4-TCNQ deposited on 2-methylpropene-modified Si(001)-2×1. This acceptor molecule increases the work function of the alkene-modified silicon surface by ∼1.3 eV after deposition of only ∼3 × 10^{14} molecules/cm^2. For the subsequent deposits in the 10^{14} molecule/cm^2 range and for the thick film (16 × 10^{14} molecules/cm^2), the work-function remains in the 5.77–5.94 eV range. On n^+-doped CP-Si(001), the deposition of TCNQ (12 × 10^{14} molecules/cm^2) makes the work function increase from 3.92 to 5.70 eV (+1.8 eV). Therefore, the work function (see Table 1) is practically equal to that of thick TCNQ layer on p^+-doped CP-Si(001), i.e., 5.77 eV. This means that the TCNQ thick-layer work function is (to less than 0.1 eV) independent of the work function of the substrate (Φ_{sub}) on which the molecule is deposited, i.e., 3.92 eV for the cyclopentene-modified n^+-substrate and 4.51 eV for the modified p^+-substrate. Therefore, the energy level alignment at the TCNQ/CP-Si(001) interface follows the ICT model,

Table 1. Variations of the Si $2p_{3/2}$ Binding Energy, $E_F - E_{VB}$, Band Bending, and Work Function as a Function of TCNQ Coverage[a]

sample	molecules/cm^2	Si $2p_{3/2}$ (eV)	silicon $E_F - E_{VB}$ (eV)	band bending (eV)	work function (eV)	HOMO centroid BE (eV)
clean silicon, p^+-doped		99.09	0.35	−0.35	5.02	
CP-Si(001), p^+-doped		99.12	0.38	−0.38	4.51	
TCNQ-CP-Si(001), p^+-doped	1.3 × 10^{14}	99.12	0.38	−0.38	5.91	
TCNQ-CP-Si(001), p^+-doped	2.0 × 10^{14}	99.27	0.53	−0.53	5.94	
TCNQ-CP-Si(001), p^+-doped	3.4 × 10^{14}	99.22	0.48	−0.48	5.808	
TCNQ-CP-Si(001), p^+-doped	**16 × 10^{14}**	**99.21**	**0.47**	**−0.47**	**5.77**	**3.4**
clean silicon, n^+-doped		99.35	0.61	0.51	4.80	
CP-Si(001), n^+-doped		99.42	0.68	0.44	3.92	
TCNQ-CP-Si(001), n^+-doped	**12 × 10^{14}**	**99.50**	**0.76**	**0.36**	**5.70**	**3.4**

[a]The HOMO BE is given for the thick films.

dx.doi.org/10.1021/jp502680b | J. Phys. Chem. C 2014, 118, 22499–22508

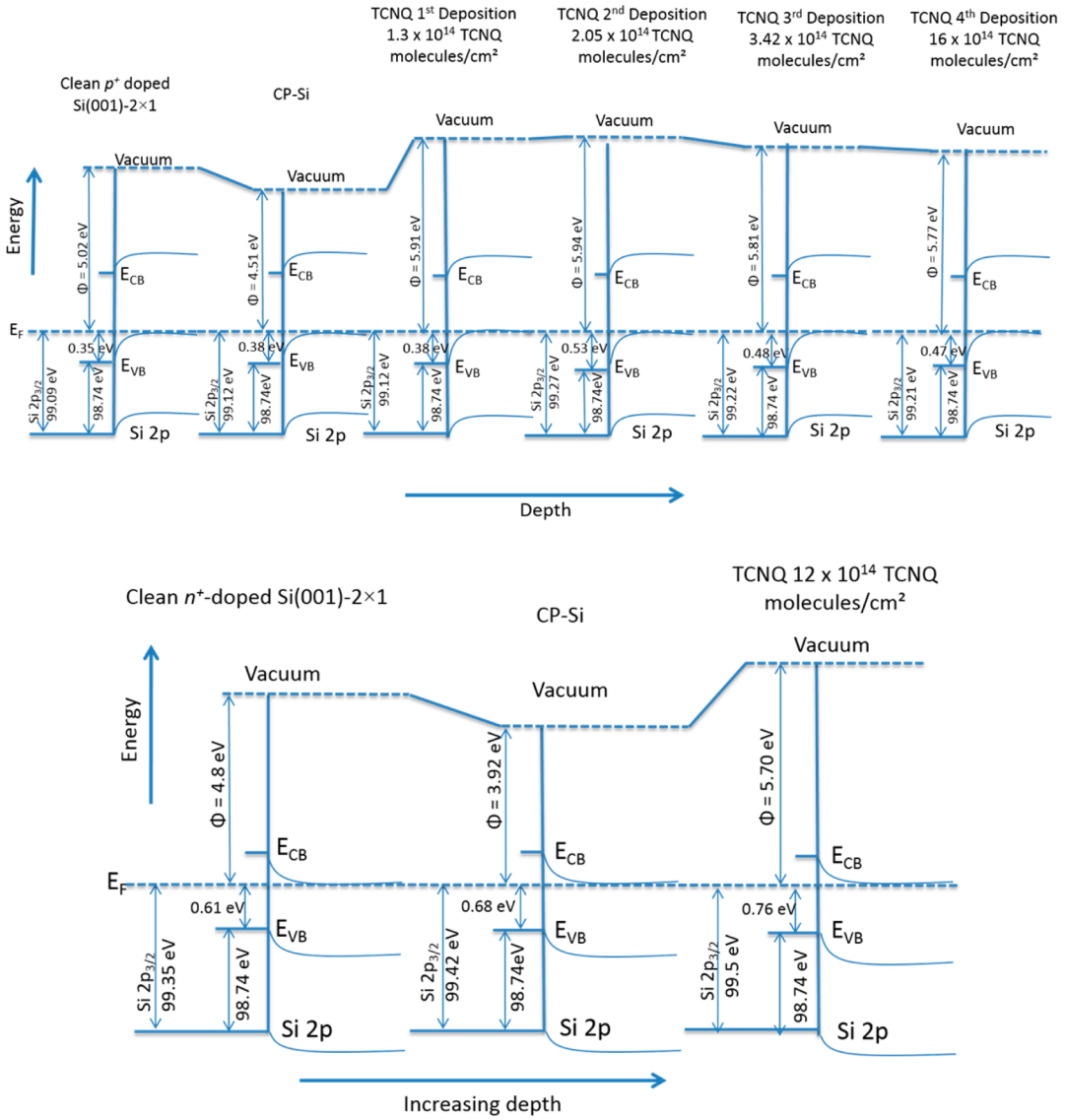

Figure 5. Energy band diagram TCNQ on CP-Si(001)-2×1: (a) p^+-doped substrate and (b) n^+-doped substrate. The $E_{VB} - E_{Si\ 2p_{3/2}}$ energy distance of 98.74 eV is taken from ref 11.

already discussed in the Introduction:[7] the Fermi level in the substrate aligns with the ICT$^-$ level of TCNQ when Φ_{sub} is smaller than ICT$^-$. In the present case ICT$^-$ *is* the measured work function, that is ∼5.7 eV, much larger than the substrate work function in the 3.9−4.5 eV range. This TCNQ ICT$^-$ of 5.70 eV is large compared to the value reported by Salaneck and co-workers, i.e., 4.8 ± 0.1 eV, collected for TCNQ on various substrates with Φ_{sub} < 4.8 eV: contaminated Au ($\Phi_{sub} \approx$ 4.0 eV),[48] AlOx (Φ_{sub} = 3.45−3.65 eV),[49] ITO (Φ_{sub} = 4.4 eV),[48] and PEDOT−PSS (Φ_{sub} = 4.6 eV).[48] However, higher work functions/ICT$^-$ are reported on substrates also fulfilling the Φ_{sub} < ICT$^-$ inequality. A value of 5.32 eV is found for TCNQ on ITO.[50] For TCNQ on H−C(001)-2×1, the ICT$^-$ level is 5.2 eV (Φ_{sub} = 4 eV).[1] For TCNQ deposited on clean Au, the work function increases from Φ_{sub} = 5.3 to 6.0 eV.[51] This dispersion in the ICT$^-$ values suggests that the Fermi level pinning energy depends on the details of the adsorption geometry at the interface. In particular the electrostatic potential step at the interface is proportional to the areal density of dipoles. The molecular crowding is larger with standing-up molecules (present situation ∼3 × 10^{14} molecules/cm^2) than with flat-lying ones (∼0.93 × 10^{14} molecules/cm^2).[52] This may explain the differences observed for the various substrates. It is also often stated that, when various acceptors are compared, the ICT$^-$ value follows that of the EA.[7] The present study shows this is not a general rule. The reported ICT$^-$ values of F4-TCNQ on *p*-doped H-C(001)-2×1 (ICT$^-$ = 5.4 eV)[1] and on AlO_x (ICT$^-$ = 5.6 eV)[46] are in fact practically equal to that of TCNQ on CP-Si(001). F4-TCNQ deposited on C_2H_4-terminated Si(001)-2×1 (Φ_{sub} = 3.9 eV) has an even smaller ICT$^-$ of 4.9 eV.[53]

The valence band and conduction band offsets can now be determined for p^+ and n^+ substrates at high coverage (taking the values collected in Table 1). The valence band offset VBO can be written as

$$\text{VBO} = E_{VB} - \text{HOMO} = (E_F - \text{HOMO}) - (E_F - E_{VB})$$

with E_F − HOMO = 3.40 eV considering the centroid, and 2.60 eV considering the edge. The conduction band offset CBO is

dx.doi.org/10.1021/jp502680b | J. Phys. Chem. C 2014, 118, 22499−22508

$$\mathrm{CBO} = E_{\mathrm{CB}} - \mathrm{LUMO}$$
$$= (E_{\mathrm{vac}} - \mathrm{LUMO}) - (E_{\mathrm{vac}} - E_{\mathrm{CB}})$$

where E_{vac} is the vacuum level energy. CBO can be rewritten as

$$\mathrm{CBO} = E_{\mathrm{vac}} - \mathrm{LUMO} - \{\Phi - (E_{\mathrm{g}} - (E_{\mathrm{F}} - E_{\mathrm{VB}}))\}$$

where E_{g} is the silicon band gap energy (1.12 eV). Inverse photoemission electron spectroscopy (IPES) measurements[54] give E_{vac} − LUMO = 3 eV considering the LUMO centroid, or 4.2 eV considering the LUMO edge. Therefore, for the TCNQ/p^+-doped CP-Si(001) interface, VBO = 2.93 eV (2.13 eV) considering the HOMO centroid (edge), and CBO = −2.12 eV (−0.92 eV) considering the LUMO centroid (edge). On the other hand, for the TCNQ/n^+-doped CP-Si(001) interface, VBO = 2.64 eV (1.84 eV) considering the HOMO centroid (edge), and CBO = −2.34 eV (−1.14 eV) considering the LUMO centroid (edge).

Possible Applications of TCNQ Ultrathin Films on an Alkene-Modified Si Surface. Recently efficient hybrid solar cells were built based on *n*-doped Si and *p*-type polymers heterostructures.[22−24] Considering that hole−electron pairs are produced by illumination in the silicon materials, holes need to be efficiently separated from electrons and injected into the *p*-type organic material. The key factors for high efficiency are (i) an upward band bending at the Si/organic interface with an electric field sweeping the holes toward the polymer, and (ii) a hole injection barrier as low as possible. A high fill factor of ∼66% and a power conversion efficiency of ∼11% were achieved for *n*-Si(111) (∼1 Ω·cm)/SiO_x (1.5 nm)/PEDOT:PSS planar stacks.[22] In this system, the upward band bending at the interface was estimated to be 0.15 eV. The SiO_x layer thickness was critical, as above 1.5 nm the efficiency diminishes due to a higher series resistance. If one considers "n^+-doped CP-Si(001)/TCNQ/hole-transporting organics", the hole−electron pair produced in silicon by illumination could be efficiently split due to the large upward band bending at the silicon surface, with a built-in potential of 0.44 eV (0.36 eV) prior to (after) TCNQ deposition. Then the strong increase in work function with respect to the pristine CP-Si(001) surface, due the deposition of TCNQ should improve the hole injection barrier. In order to optimally use the work function increase provided by TCNQ deposition, the hole-conducting layer should align its vacuum level with that of TCNQ (Schottky−Mott limit).[55] This would require that the positive ICT (ICT$^+$) level of the hole-conducting material would be greater than the ICT$^-$ level of TCNQ.[56] Hole conductors with a high ICT$^+$ may not be that common. For instance, Braun et al.[55] reported on CBP (4,4′-*N*,*N*′-dicarbazolyl-biphenyl) that has an ICT$^+$ of ∼5.2 eV, close to but still smaller than the ICT$^-$ of TCNQ. In a recent work on the C_2H_4−Si(001)/F4-TCNQ/pentacene stacking,[5,53] no vacuum-level alignment between F4-TCNQ and pentacene was observed. In fact there is no surprise, as pentacene has an ICT$^+$ of 4.2 eV,[57] smaller than the ICT$^-$ level of F4-TCNQ (4.9 eV in ref 53). However, despite a drop in the work function at the F4-TCNQ/pentacene interface, a net improvement (by 0.6−0.8 eV) of the hole injection barrier was obtained when compared to the C_2H_4−Si(001)/pentacene stack.

CONCLUSION

We have measured changes of the surface work function (via secondary electron cutoff measurement), band-bending variations at the p^+- and n^+-doped CP-Si(001) (via surface sensitive Si 2p XPS), and possible changes in the chemistry of TCNQ (via N 1s XPS/NEXAFS) as a function of increasing surface density of deposited TCNQ molecules, from (sub)monolayer deposits (∼10^{14} molecules/cm^2 range) to thick layers (∼10^{15} molecules/cm^2 range) on the p^+-doped substrate. Only a thick layer (∼10^{15} molecules/cm^2) was deposited on the n^+-doped substrate.

With respect to clean reconstructed silicon, the CP-Si(001) surfaces are characterized by a sizable decrease of the work function (that may be detrimental to some application). Si 2p XPS also shows that flat band conditions are not reached due to the presence of electrically active defects (donors and acceptors) at the interface with a density greater than 10^{-3} ML.

For p^+-doped CP-Si(001), the N 1s XPS and NEXAFS spectral shape at (sub)monolayer coverage is strikingly different from that of the thick layer (made of neutral molecules $TCNQ^0$). The formation of an anionic species at (sub)-monolayer coverage, the filling of the LUMO, and the aromatization of the central ring are indicated by the *absence* of the 1s-to-central ring transition at $h\nu$ = 397 eV in the NEXAFS N 1s spectra that is observed for $TCNQ^0$. The LUMO filling is further confirmed by the absence of the π-to-π^* shakeup in the N 1s XPS spectra. For their part, the (sub)monolayer N 1s XPS spectra exhibit two components at ∼399.9 and ∼398.5 eV, while $TCNQ^0$ in the thick film exhibits a main N 1s XPS peak at a binding energy of ∼399.6 eV. As a mixture of anionic and neutral molecules in the (sub)-monolayer range is not supported by NEXAFS, we propose that the molecule is asymmetrically charged: the cyano groups directed toward the modified surface would become negatively charged (low binding energy component), while those protruding into the vacuum would remain neutral (high binding energy component). This hypothesis is all the more sensible, considering that the NEXAFS spectra of (sub)-monolayer molecules indicate that the molecule stands up on the surface.

We note that the huge increase in work function from 4.5 eV (pristine p^+ CP-Si(001)) to ∼5.8 ± 0.1 eV *is already obtained at (sub)monolayer coverage* (10^{14} molecules/cm^2), which also lends strength to the presence of negatively charged TCNQ molecules on CP-Si(001)-2×1. The effect has the same amplitude as that found for F4-TCNQ on ethylene-modified Si(001), although TCNQ is a less strong electron acceptor than F4-TCNQ.

We also observe that the positioning of the Fermi level at the cyclopentene/Si interface remains blocked due to electrically active defects resulting from the alkene passivation, in contrast to the unpinned behavior of H-terminated C(001)-2×1.[2] The nature of the dipolar layer between $TNCQ^-$ and some undefined donor levels residing within the top layers of CP-Si(001)-2×1 remains to be understood. When the deposited TCNQ amounts are 1 order of magnitude greater (10^{15} molecules/cm^2 range), XPS and NEXAFS spectra are characteristic of the neutral molecule, where the NEXAFS study further indicates a change in molecular orientation, from standing up to recumbent (the molecular plane makes an angle of about 36° with the surface place).

The comparison of extreme p^+ and n^+ doping levels was thought to be a means to vary the work functions of CP-Si(001)-2×1 surfaces in a wide energy interval, i.e., between 4.5 eV (p^+) and 3.9 eV (n^+). In both cases the work function of thick films (10^{15} molecules/cm^2 range) was equal to ∼5.7 eV.

dx.doi.org/10.1021/jp502680b | J. Phys. Chem. C 2014, 118, 22499−22508

We reason that, as the work function of the substrate in both cases is smaller than that of the molecular layer, the Fermi level is pinned to a negative integer charge-transfer state, resulting in an organic layer work function independent of the substrate. This study is therefore a further confirmation of Salaneck's Integer Charge Transfer (ITC) model, leading to a negative ICT energy (ICT^-) of ~5.7 eV. We also conclude that the relative dispersion of TCNQ ICT^- values in the literature (from 4.8 to 6 eV) may be due to a different molecular stacking at the interface.

From the application point of view, our presentation of the energy level schemes of the TCNQ/CP-Si(001)-2×1 system gives estimates of the hole and electron injection barriers for both doping levels. The possible use of a TCNQ (sub)-monolayer to improve the hole injection barrier in CP-Si(001)/TCNQ/hole-conductor stacks is examined.

■ ASSOCIATED CONTENT

Supporting Information

Methodology adopted to estimate TCNQ coverage, measurement of work function using the secondary electron cutoff, additional NEXAFS spectra of an n^+-doped CP-Si(001)-2×1, determination of molecular orientation via NEXAFS, and the difference curve between valence band spectra of TCNQ-CP-Si(001) and the pristine substrate. This material is available free of charge via the Internet at http://pubs.acs.org.

■ AUTHOR INFORMATION

Corresponding Author

*E-mail: francois.rochet@upmc.fr.

Author Contributions

The LCPMR team designed the study, developed the methodology, collected the data, performed the analysis, and wrote the manuscript. The SOLEIL team gave a substantial contribution to instrumental development and data acquisition and collection.

Notes

The authors declare no competing financial interest.

■ ACKNOWLEDGMENTS

A.K. gratefully acknowledges the funding received toward his Ph.D. from the UPMC fellowship (Ecole Doctorale ED388).

■ ABBREVIATIONS

CP-Si(001)-2×1, cyclopentene-modified Si(001) surface; EA, electron affinity; E_{VB}, valence band maximum; fwhm, full width at half-maximum; HOMO, highest occupied molecular orbital; ICT, integer charge transfer; IP, ionization potential; ISC, inorganic semiconductors; LUMO, lowest unoccupied molecular orbital; ML, monolayer; NEXAFS, near-edge X-ray absorption fine structure; TCNQ, tetracyanoquinodimethane; UPS, ultraviolet photoelectron spectroscopy; XPS, X-ray photoelectron spectroscopy

■ REFERENCES

(1) Chen, W.; Qi, D.; Gao, X.; Wee, A. T. S. Surface Transfer Doping of Semiconductors. *Prog. Surf. Sci.* **2009**, *84*, 279−321.

(2) Qi, D.; Chen, W.; Gao, X.; Wang, L.; Chen, S.; Loh, K. P.; Wee, A. T. S. Surface Transfer Doping of Diamond (100) by Tetrafluoro-Tetracyanoquinodimethane. *J. Am. Chem. Soc.* **2007**, *129*, 8084−8085.

(3) Furuhashi, M.; Yoshinobu, J. Charge Transfer and Molecular Orientation of Tetrafluoro-Tetracyanoquinodimethane on a Hydrogen-Terminated Si(111) Surface Prepared by a Wet Chemical Method. *J. Phys. Chem. Lett.* **2010**, *1*, 1655−1659.

(4) Mukai, K.; Yoshinobu, J. Observation of Charge Transfer States of F4-TCNQ on the 2-Methylpropene Chemisorbed Si(100)(2×1) Surface. *J. Electron Spectrosc. Relat. Phenom.* **2009**, *174*, 55−58.

(5) Yoshimoto, S.; Kameshima, K.; Koitaya, T.; Harada, Y.; Mukai, K.; Yoshinobu, J. Interface State and Energy Level Alignment of F4-TCNQ Sandwiched between a Pentacene Film and the Ethylene-Terminated Si(100) Surface. *Org. Electron.* **2014**, *15*, 356−364.

(6) Dubey, G.; Rosei, F.; Lopinski, G. P. Highly Sensitive Electrical Detection of TCNE on Chemically Passivated Silicon-on-Insulator. *Chem. Commun. (Camb.)* **2011**, *47*, 10593−10595.

(7) Braun, S.; Salaneck, W. R.; Fahlman, M. Energy-Level Alignment at Organic/Metal and Organic/Organic Interfaces. *Adv. Mater.* **2009**, *21*, 1450−1472.

(8) Bokdam, M.; Çakır, D.; Brocks, G. Fermi Level Pinning by Integer Charge Transfer at Electrode-Organic Semiconductor Interfaces. *Appl. Phys. Lett.* **2011**, *98*, 113303.

(9) Maier, F.; Riedel, M.; Mantel, B.; Ristein, J.; Ley, L. Origin of Surface Conductivity in Diamond. *Phys. Rev. Lett.* **2000**, *85*, 3472−3475.

(10) Himpsel, F. J.; Meyerson, B. S.; Mc Feely, I. R.; Morar, J. F.; Taleb-Ibrahimi, A.; Yarmoff, J. A. Core Level Spectroscopy at Silicon Surfaces and Interfaces. In *Proceedings of the Enrico Fermi School on Photoemission and Absorption Spectroscopy of Solids and Interfaces with Synchrotron Radiation*; Campagna, M., Rosei, R., Eds.; North Holland: Amsterdam, 1988; pp 203−236.

(11) Himpsel, F. J.; Hollinger, G.; Pollak, R. A. Determination of the Fermi-Level Pinning Position at Si(111)surfaces. *Phys. Rev. B* **1983**, *28*, 7014−7018.

(12) Zur, A.; McGill, T.; Smith, D. Fermi-Level Position at a Semiconductor-Metal Interface. *Phys. Rev. B* **1983**, *28*, 2060−2067.

(13) Gao, W.; Kahn, A. Electronic Structure and Current Injection in Zinc Phthalocyanine Doped with Tetrafluorotetracyanoquinodimethane: Interface versus Bulk Effects. *Org. Electron.* **2002**, *3*, 53−63.

(14) Sato, N.; Seki, K.; Inokuchi, H. Polarization Energies of Organic Solids Determined by Ultraviolet Photoelectron Spectroscopy. *J. Chem. Soc., Faraday Trans. 2* **1981**, *77*, 1621.

(15) Aristov, V. Y.; Le Lay, G.; Hricovini, K.; Taleb-Ibrahimi, A.; Dumas, P.; Gunther, R.; Osvald, J.; Indlekofer, G. Nearly Complete Tuning of the Fermi Level Position at a Prototypical Metal-Silicon Interface: Lead on Unpinned Si(111)1×1-H. *J. Electron Spectrosc. Relat. Phenom.* **1994**, *68*, 419−426.

(16) Buriak, J. M. Organometallic Chemistry on Silicon and Germanium Surfaces. *Chem. Rev.* **2002**, *102*, 1271−1308.

(17) Hunger, R.; Fritsche, R.; Jaeckel, B.; Jaegermann, W.; Webb, L.; Lewis, N. Chemical and Electronic Characterization of Methyl-Terminated Si(111) Surfaces by High-Resolution Synchrotron Photoelectron Spectroscopy. *Phys. Rev. B* **2005**, *72*.

(18) Hamers, R. J.; Hovis, J. S.; Lee, S.; Liu, H.; Shan, J. Formation of Ordered, Anisotropic Organic Monolayers on the Si(001) Surface. *J. Phys. Chem. B* **1997**, *101*, 1489−1492.

(19) Bent, S. F. Attaching Organic Layers to Semiconductor Surfaces. *J. Phys. Chem. B* **2002**, *106*, 2830−2842.

(20) Khaliq, A.; Pierucci, D.; Tissot, H.; Gallet, J.-J.; Bournel, F.; Rochet, F.; Silly, M.; Sirotti, F. Ene-Like Reaction of Cyclopentene on Si(001)-2×1: An XPS and NEXAFS Study. *J. Phys. Chem. C* **2012**, *116*, 12680−12686.

(21) Weidkamp, K. P.; Hacker, C. A.; Schwartz, M. P.; Cao, X.; Tromp, R. M.; Hamers, R. J. Interfacial Chemistry of Pentacene on Clean and Chemically Modified Silicon (001) Surfaces. *J. Phys. Chem. B* **2003**, *107*, 11142−11148.

(22) He, L.; Jiang, C.; Wang, H.; Lai, D. High Efficiency Planar Si/organic Heterojunction Hybrid Solar Cells. *Appl. Phys. Lett.* **2012**, *100*, No. 073503.

(23) Zhu, Y.; Song, T.; Zhang, F.; Lee, S.-T.; Sun, B. Efficient Organic-Inorganic Hybrid Schottky Solar Cell: The Role of Built-in Potential. *Appl. Phys. Lett.* **2013**, *102*, No. 113504.

(24) Fan, X.; Zhang, M.; Wang, X.; Yang, F.; Meng, X. Recent Progress in Organic−inorganic Hybrid Solar Cells. *J. Mater. Chem. A* **2013**, *1*, 8694.
(25) Yamashita, Y.; Nagao, M.; Machida, S.; Hamaguchi, K.; Yasui, F.; Mukai, K.; Yoshinobu, J. High Resolution Si 2p Photoelectron Spectroscopy of Unsaturated Hydrocarbon Molecules Adsorbed on Si(100)c(4×2): The Interface Bonding and Charge Transfer between the Molecule and the Si Substrate. *J. Electron Spectrosc. Relat. Phenom.* **2001**, *114*−*116*, 389−393.
(26) Mathieu, C.; Bai, X.; Bournel, F.; Gallet, J.-J.; Carniato, S.; Rochet, F.; Sirotti, F.; Silly, M.; Chauvet, C.; Krizmancic, D. Nitrogen 1s NEXAFS and XPS Spectroscopy of NH_3-Saturated Si(001)-2×1: Theoretical Predictions and Experimental Observations at 300 K. *Phys. Rev. B* **2009**, *79*, No. 205317.
(27) Stöhr, J. *NEXAFS Spectroscopy*; Springer: NewYork, 1992; pp 158−159.
(28) Himpsel, F.; McFeely, F.; Taleb-Ibrahimi, A.; Yarmoff, J.; Hollinger, G. Microscopic Structure of the SiO2/Si Interface. *Phys. Rev. B* **1988**, *38*, 6084−6096.
(29) Carniato, S.; Gallet, J.-J.; Rochet, F.; Dufour, G.; Bournel, F.; Rangan, S.; Verdini, A.; Floreano, L. Characterization of Hydroxyl Groups on Water-Reacted Si(001)-2×1 Using Synchrotron Radiation O 1s Core-Level Spectroscopies and Core-Excited State Density-Functional Calculations. *Phys. Rev. B* **2007**, *76*, No. 085321.
(30) Zhang, Q.; Kong, L.; Zhang, Q.; Wang, W.; Hua, Z. The Effect of Heat Treatment on Bistable Ag-TCNQ Thin Films. *Solid State Commun.* **2004**, *130*, 799−802.
(31) Medjanik, K.; Gloskovskii, A.; Kutnyakhov, D.; Felser, C.; Chercka, D.; Baumgarten, M.; Müllen, K.; Schönhense, G. Charge Transfer in the Novel Donor−acceptor Complexes Tetra- and Hexamethoxypyrene with Tetracyanoquinodimethane Studied by HAXPES. *J. Electron Spectrosc. Relat. Phenom.* **2012**, *185*, 77−84.
(32) Lindquist, J. M.; Hemminger, J. C.; Lindquist, J. M. High-Resolution Core Level Photoelectron Spectra of Solid TCNQ: Determination of Molecular Orbital Spatial Distribution from Localized Shake-up Features. *J. Phys. Chem.* **1988**, *92*, 1394−1396.
(33) Fraxedas, J.; Lee, Y.; Jiménez, I.; Gago, R.; Nieminen, R.; Ordejón, P.; Canadell, E. Characterization of the Unoccupied and Partially Occupied States of TTF-TCNQ by XANES and First-Principles Calculations. *Phys. Rev. B* **2003**, *68*, No. 195115.
(34) Aarons, L. J.; Barber, M.; Connor, J. A.; Guest, M. F.; Hillier, I. H.; Ikemoto, I.; Thomas, J. M.; Kuroda, H. Satellite Phenomena in the High Energy Photoelectron Spectra of Tetramethyl-P-Phenylenediamine (TMPD), Tetracyanoquinodimethane (TCNQ), and Their Derivatives. Experimental and Theoretical Study. *J. Chem. Soc., Faraday Trans. 2* **1973**, *69*, 270.
(35) Giergiel, J.; Wells, S.; Land, T. A.; Hemminger, J. C. Growth and Chemistry of TCNQ Films on Nickel (111). *Surf. Sci.* **1991**, *255*, 31−40.
(36) Tseng, T.-C.; Urban, C.; Wang, Y.; Otero, R.; Tait, S. L.; Alcamí, M.; Ecija, D.; Trelka, M.; Gallego, J. M.; Lin, N.; et al. Charge-Transfer-Induced Structural Rearrangements at Both Sides of Organic/metal Interfaces. *Nat. Chem.* **2010**, *2*, 374−379.
(37) Coletti, C.; Riedl, C.; Lee, D. S.; Krauss, B.; Patthey, L.; von Klitzing, K.; Smet, J. H.; Starke, U. Band Structure Engineering of Epitaxial Graphene on SiC by Molecular Doping. *Phys. Rev. B* **2010**, *81*, No. 235401.
(38) Medjanik, K.; Chercka, D.; Nagel, P.; Merz, M.; Schuppler, S.; Baumgarten, M.; Müllen, K.; Nepijko, S. a; Elmers, H.-J.; Schönhense, G.; et al. Orbital-Resolved Partial Charge Transfer from the Methoxy Groups of Substituted Pyrenes in Complexes with Tetracyanoquinodimethane-A NEXAFS Study. *J. Am. Chem. Soc.* **2012**, *134*, 4694−4699.
(39) Hua, Weijie; Gao Bin, L. Y. First-Principle Simulation of Soft X-Ray Spectroscopy. *Prog. Chem.* **2012**, *24*, 964−980.
(40) Stöhr, J. *NEXAFS Spectroscopy*; Springer: NewYork, 1992; p 284.
(41) Milián, B.; Pou-Amérigo, R.; Viruela, R.; Ortí, E. On the Electron Affinity of TCNQ. *Chem. Phys. Lett.* **2004**, *391*, 148−151.
(42) Chen, W.; Chen, S.; Qi, D. C.; Gao, X. Y.; Wee, A. T. S. Surface Transfer P-Type Doping of Epitaxial Graphene. *J. Am. Chem. Soc.* **2007**, *129*, 10418−10422.
(43) Koch, N.; Duhm, S.; Rabe, J.; Vollmer, A.; Johnson, R. Optimized Hole Injection with Strong Electron Acceptors at Organic-Metal Interfaces. *Phys. Rev. Lett.* **2005**, *95*, No. 237601.
(44) Grobman, W.; Pollak, R.; Eastman, D.; Maas, E.; Scott, B. Valence Electronic Structure and Charge Transfer in Tetrathiofulvalinium Tetracyanoquinodimethane (TTF-TCNQ) from Photoemission Spectroscopy. *Phys. Rev. Lett.* **1974**, *32*, 534−537.
(45) Lin, S.; Spicer, W.; Schechtman, B. Electron Escape Depth, Surface Composition, and Charge Transfer in Tetrathiafulvalene Tetracyanoquinodimethane (TTF-TCNQ) and Related Compounds: Photoemission Studies. *Phys. Rev. B* **1975**, *12*, 4184−4199.
(46) Braun, S.; Salaneck, W. R. Fermi Level Pinning at Interfaces with Tetrafluorotetracyanoquinodimethane (F4-TCNQ): The Role of Integer Charge Transfer States. *Chem. Phys. Lett.* **2007**, *438*, 259−262.
(47) Masuda, S.; Hayashi, H.; Harada, Y.; Kato, S. Penning-Ionization Electron Spectroscopy of Tetrafluoro-TCNQ Anion without Counter Ion Prepared on Graphite. *Chem. Phys. Lett.* **1991**, *180*, 279−282.
(48) Murdey, R. J.; Salaneck, W. R. Charge Injection Barrier Heights Across Multilayer Organic Thin Films. *Jpn. J. Appl. Phys.* **2005**, *44*, 3751−3756.
(49) Braun, S.; Liu, X.; Salaneck, W. R.; Fahlman, M. Fermi Level Equilibrium at Donor−acceptor Interfaces in Multi-Layered Thin Film Stack of TTF and TCNQ. *Org. Electron.* **2010**, *11*, 212−217.
(50) Mayer, T.; Hein, C.; Härter, J.; Mankel, E.; Jaegermann, W. A Doping Mechanism for Organic Semiconductors Derived from SXPS Measurements on Co-Evaporated Films of CuPc and TCNQ and on a TCNQ/CuPc Interface. In *Organic Photovoltaics IX*, Proceedings of SPIE *7052*, San Diego, CA, Aug 10, 2008; Kafafi, Z. H., Lane, P. A., Eds.; International Society for Optics and Photonics: Bellingham, WA, 2008; No. 705204.
(51) Medjanik, K.; Perkert, S.; Naghavi, S.; Rudloff, M.; Solovyeva, V.; Chercka, D.; Huth, M.; Nepijko, S.; Methfessel, T.; Felser, C. Formation of an Intermolecular Charge-Transfer Compound in UHV Codeposited Tetramethoxypyrene and Tetracyanoquinodimethane. *Phys. Rev. B* **2010**, *82*, No. 245419.
(52) Qi, Y.; Mazur, U.; Hipps, K. W. Charge Transfer Induced Chemical Reaction of Tetracyano-P-Quinodimethane Adsorbed on Graphene. *RSC Adv.* **2012**, *2*, 10579.
(53) Yoshinobu, J.; Kameshima, K.; Mukai, K.; Yoshimoto, S. Thin Film Pentacene on the Chemically Modified Si(100) Surfaces: Growth, Energy Level Alignment and Electronic States. Presented at the 6th Japan-Sweden Workshop on Advanced Spectroscopy of Organic Materials for Electronic Applications (ASOMEA-VI); Kaga-Onsen, Ishikawa, Japan, Nov 23−26, 2011.
(54) Kanai, K.; Akaike, K.; Koyasu, K.; Sakai, K.; Ouchi, Y.; Seki, K.; Nishi, T. Determination of Electron Affinity of Electron Accepting Molecules. *Appl. Phys. A: Mater. Sci. Process.* **2009**, *95*, 309−313.
(55) Braun, S.; Osikowicz, W.; Wang, Y.; Salaneck, W. Energy Level Alignment Regimes at Hybrid Organic−organic and Inorganic−organic Interfaces. *Org. Electron.* **2007**, *8*, 14−20.
(56) Meyer zu Heringdorf, F. J.; Reuter, M. C.; Tromp, R. M. Growth Dynamics of Pentacene Thin Films. *Nature* **2001**, *412*, 517−520.
(57) Koch, N.; Elschner, A.; Rabe, J. P.; Johnson, R. L. Work Function Independent Hole-Injection Barriers Between Pentacene and Conducting Polymers. *Adv. Mater.* **2005**, *17*, 330−335.